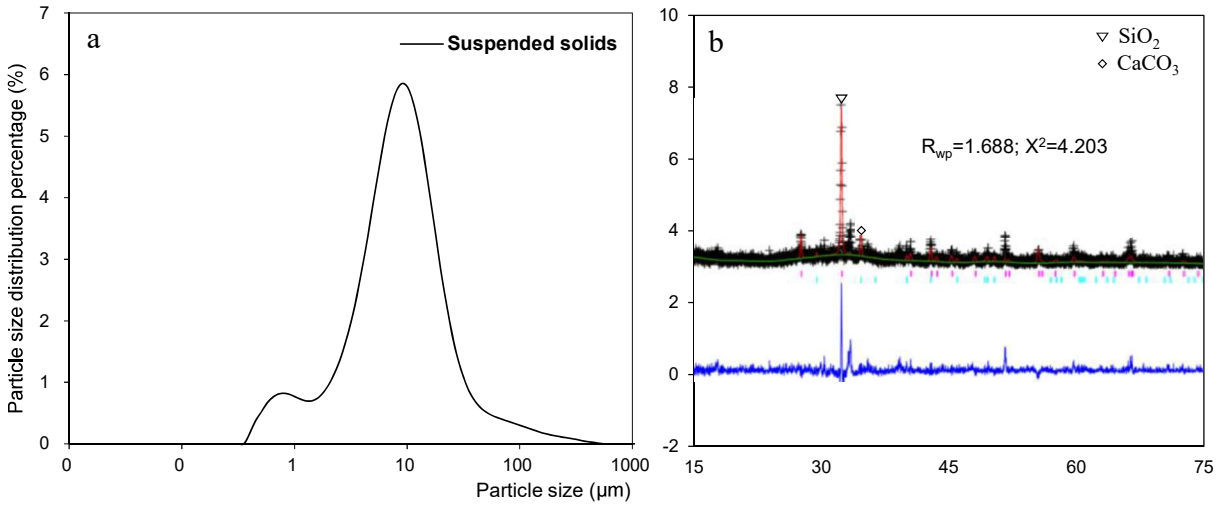

Fig. 1. Suspended particle size distribution and mineral composition. (a) Size distribution of suspended particles. (b) X-ray diffraction (XRD) pattern of suspended particles.

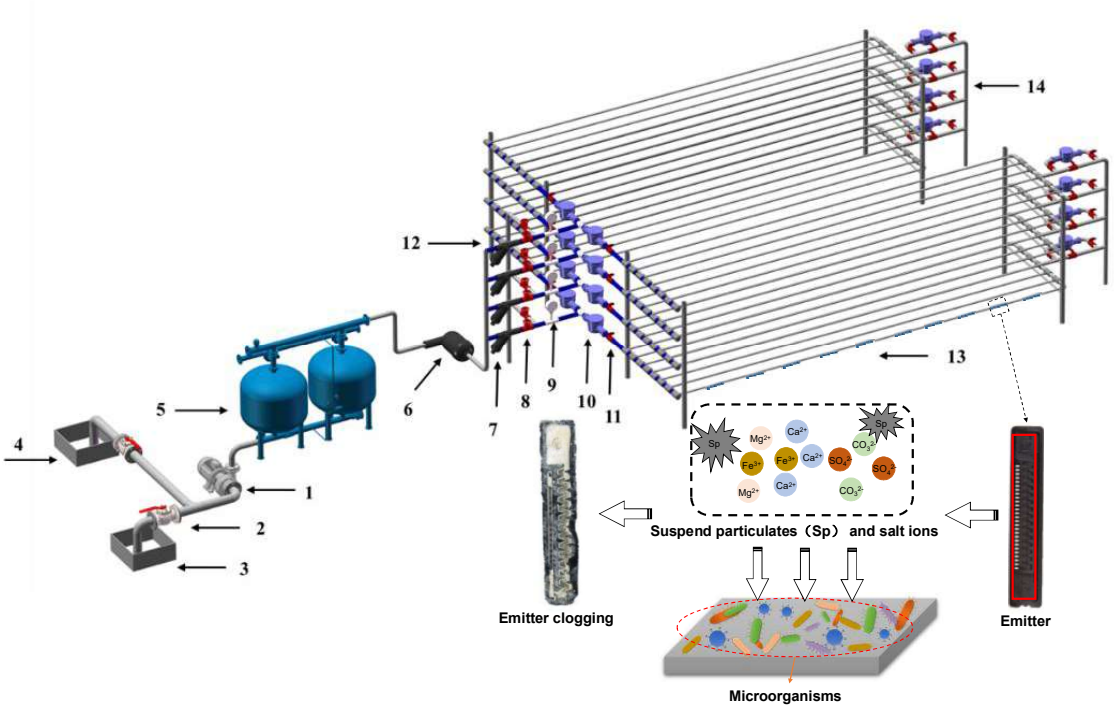

15

16 **Fig. 2. Layout of drip irrigation experimental system.** 1, water pump; 2, butterfly valve; 3, fertilizer pond; 4, water pond;
17 5, sand filter; 6, disc filter; 7, small disc filter; 8, copper valve; 9, pressure gauge; 10, water meter; 11, small ball valve; 12,
18 return pipe; 13, drip irrigation pipe; 14, flushing valve.

19

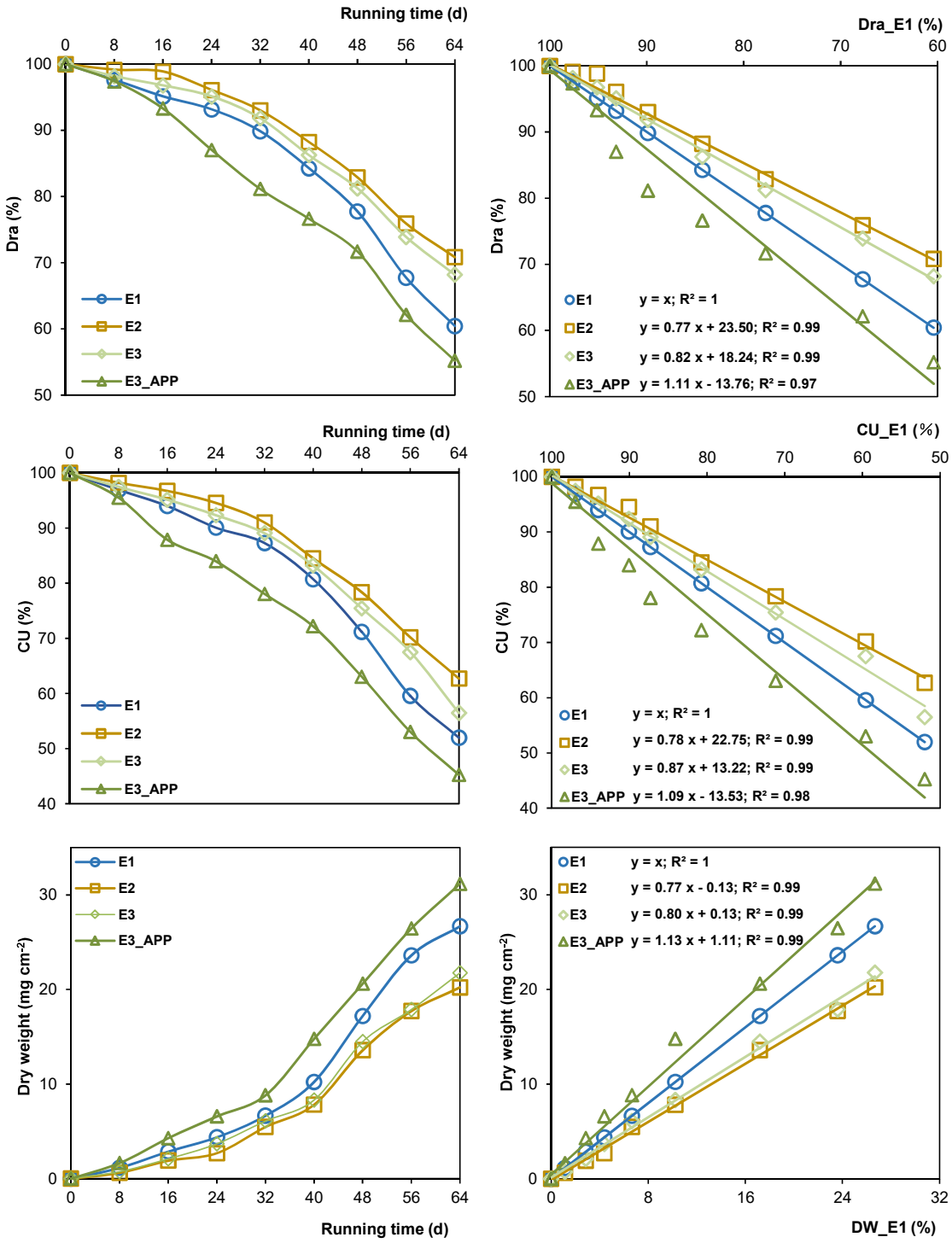

Fig. 3. Dynamic changes of emitter performance and clogging substance content between different treatments

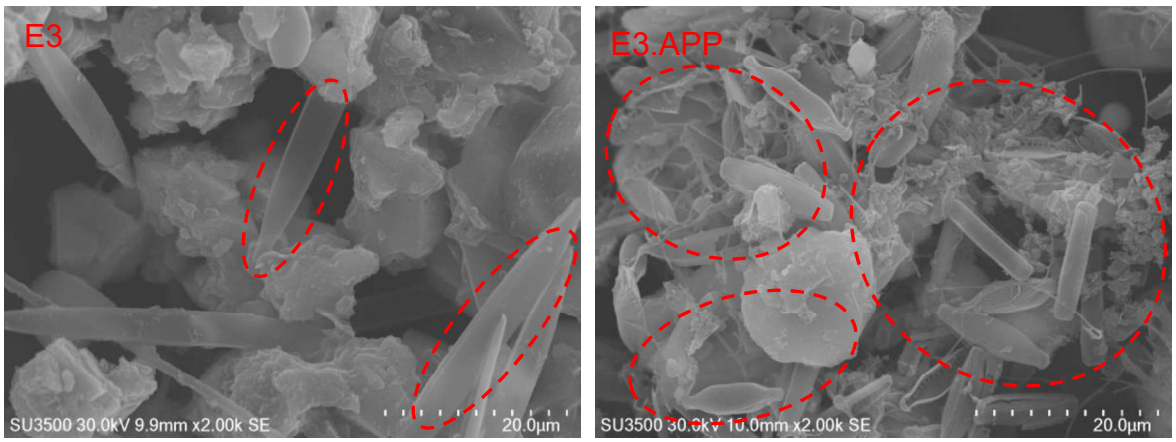

Fig. 4. Scanning electron microscope images of fouling (scale bar 20µm)

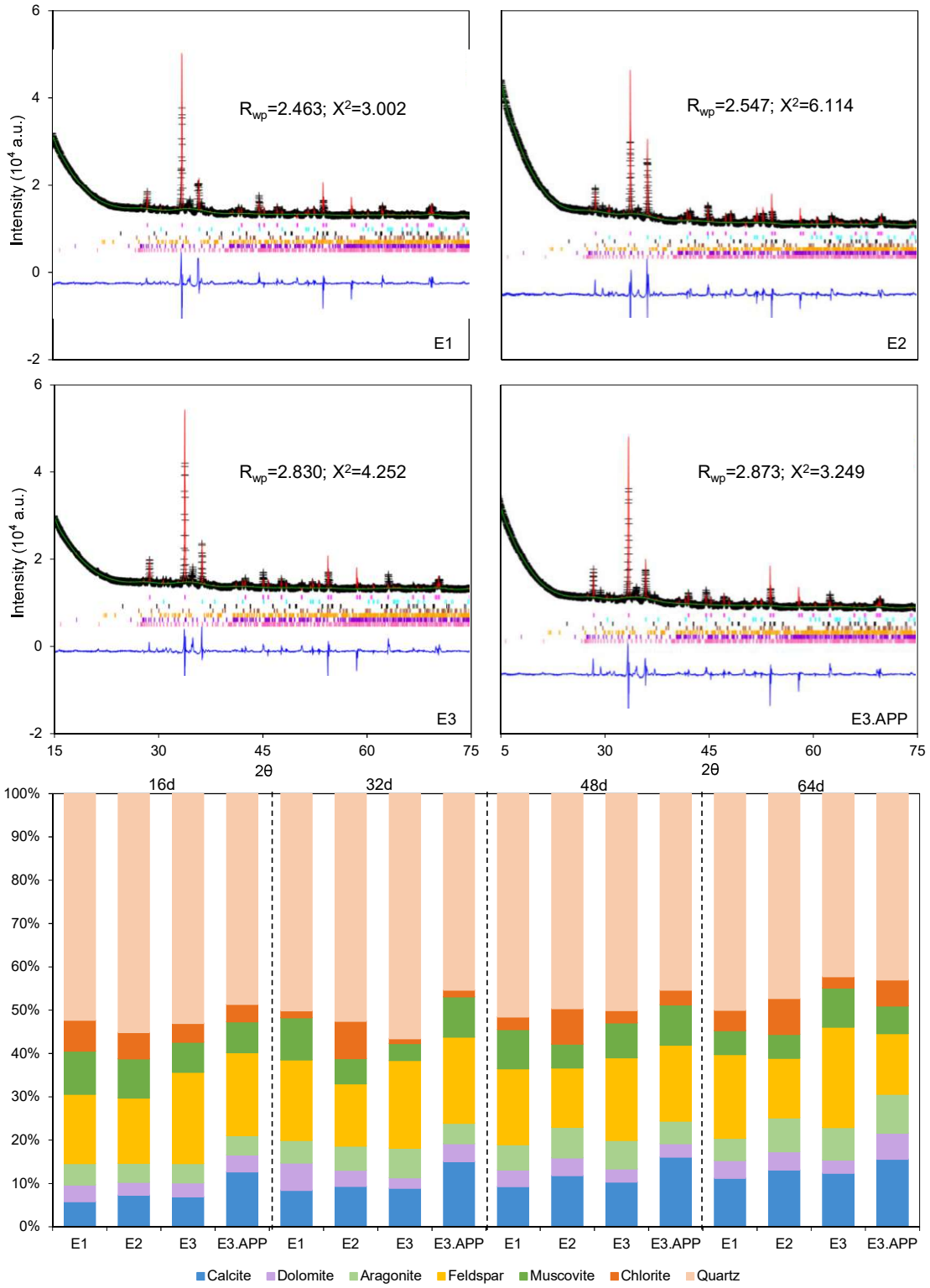

Fig. 5. Mineral composition and relative proportion of particulates and precipitates inside emitters

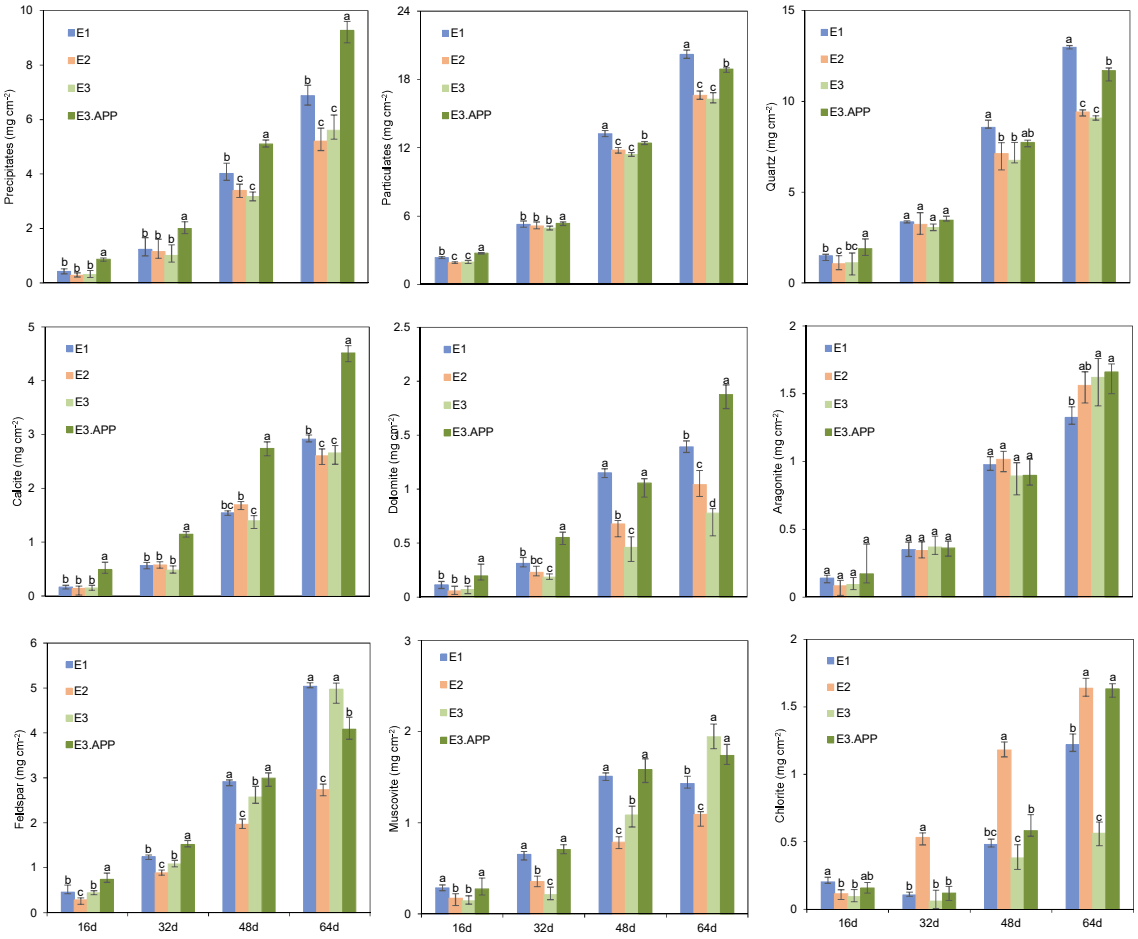

Fig. 6. Average variation of mineral contents with respect to time. Bars are standard errors. Values without the same letters within the same column at each sampling day are significantly different ($p < 0.05$).

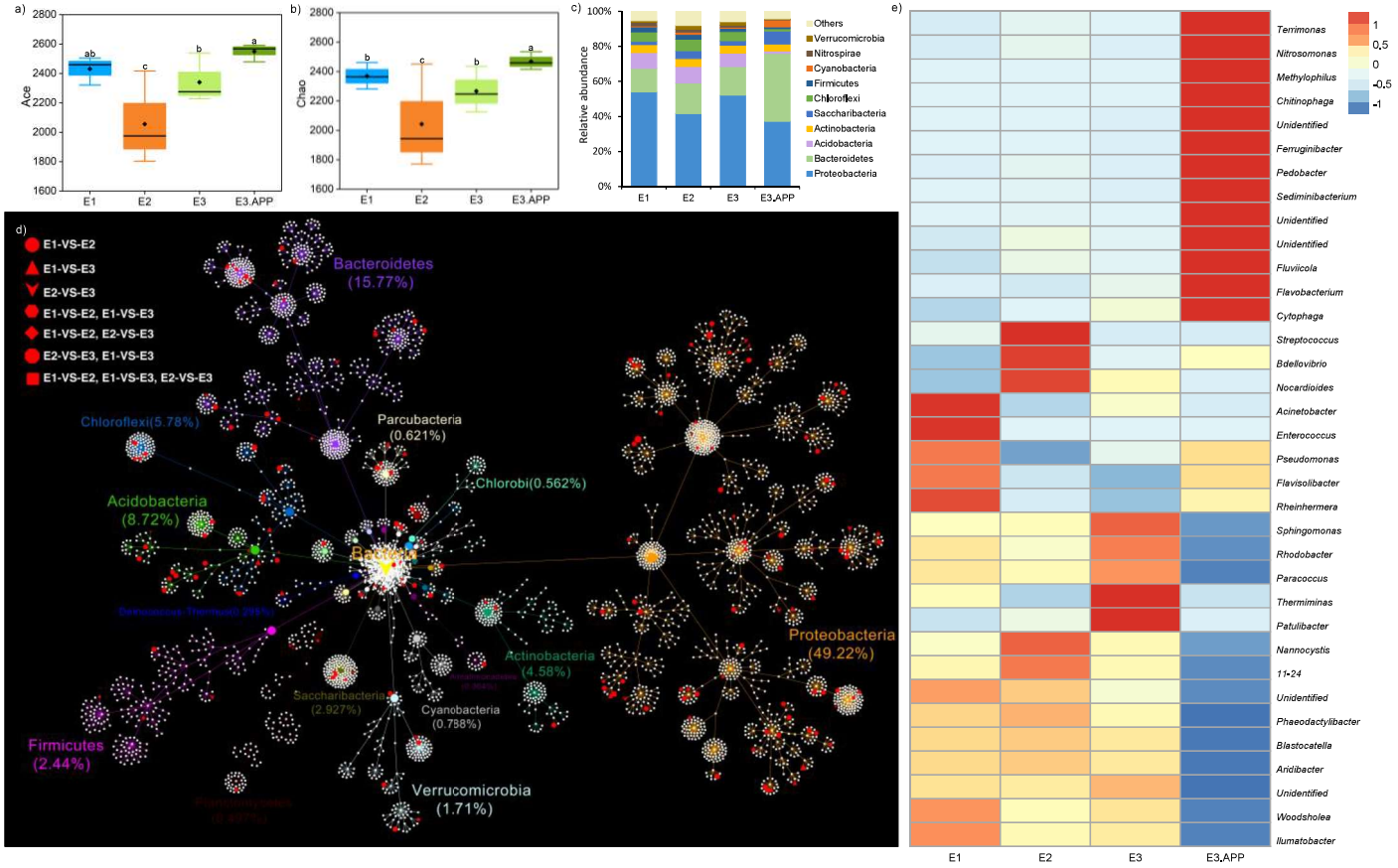

Fig. 7. The diversity index and taxonomic composition of the bacterial communities. (a-b) Variation of the diversity index. The values of Ace and Chao can reflect the richness and diversity of microbial community in samples. Bars are standard errors. (c) Bacteria taxonomic composition at the phylum level (top10). (d) Dendrogram of the microbial communities. The most abundant phyla were marked with different colors. The percentages in brackets were the relative abundances of the corresponding phyla. The white node in the figure represents that the difference in OTU is not significant, and the red node represents that the difference in OTU is significant ($p < 0.05$). (e) The clustering abundance information of species (top35).

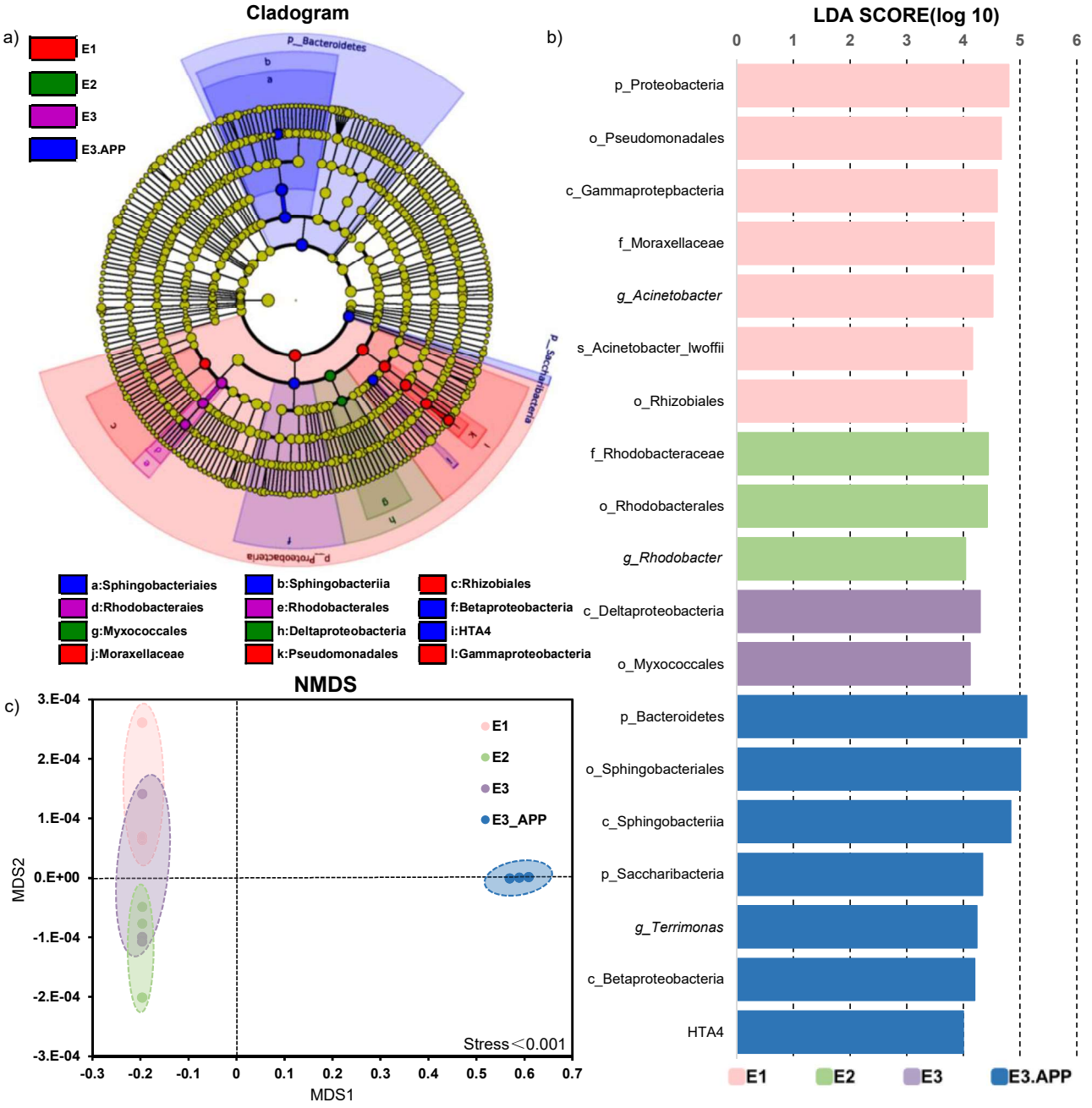

Fig. 8. Biomarker analysis between groups. (a) Linear discriminant analysis effect size (LEFSe) cladogram. The categorization level from the phylum to the genus is represented by the circle radiating from the interior to the outside, and the size of the circle is proportional to the relative abundance. The red, green, purple, and blue nodes represent the microbial groups that play important roles in E1, E2, E3, and E3.APP, respectively. The yellow node represents that there was no significant difference in species at this level. (b) Linear discriminant analysis (LDA) histogram. The extent of the difference in the biomarker is represented by the length of the histogram, and a length larger than 4 indicates that the difference is significant. (c) Analysis of bacterial community structure by non-metric multidimensional scaling (NMDS).

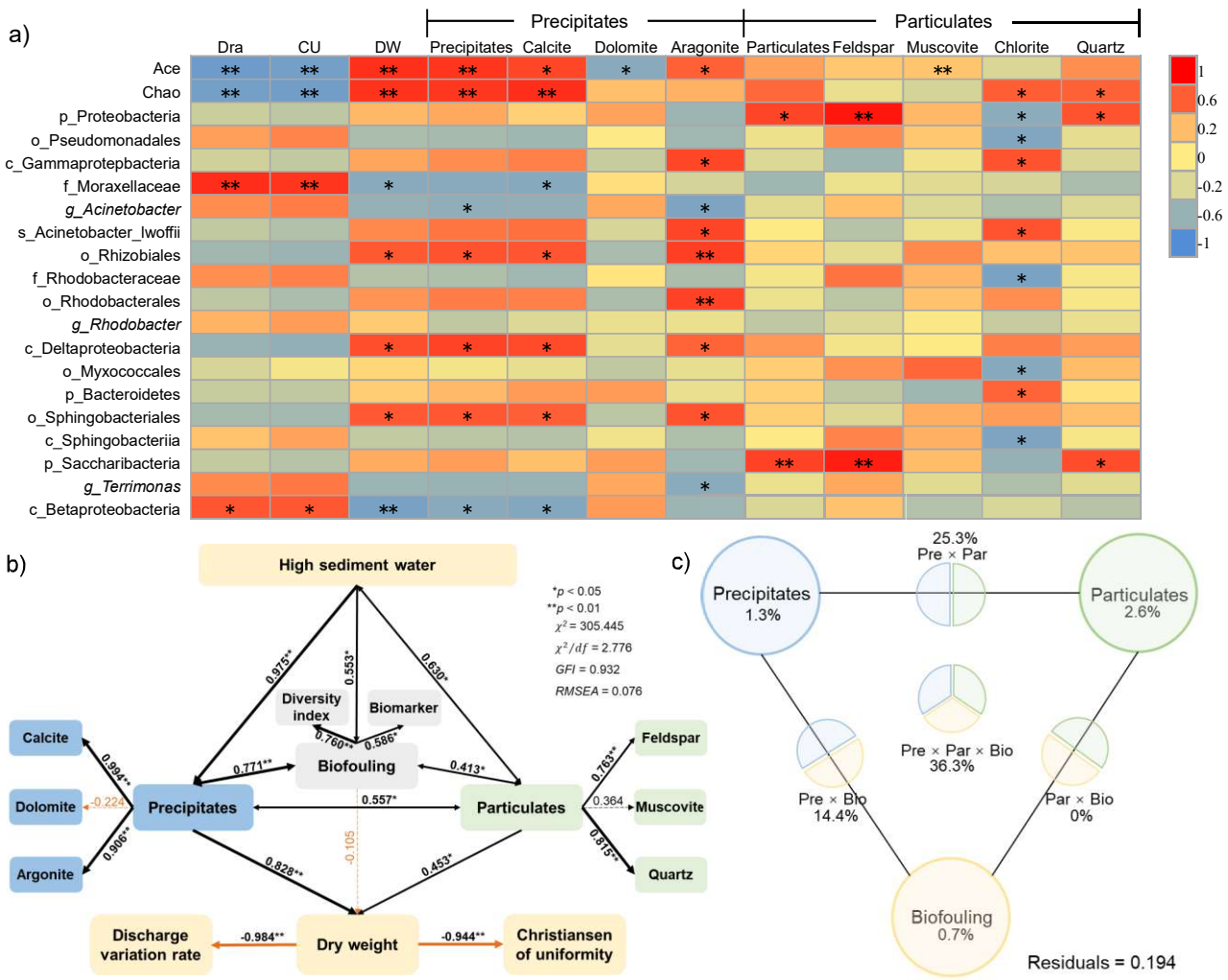

Fig. 9. Interaction between composite fouling. (a) Spearman correlation analysis of emitter performance index and composite fouling. (b) Structural equation modeling analysis (SEMA). The number between two modules is the standard path coefficient (γ). The color indicates a positive impact (black) or a negative impact (orange), and the solid and dotted lines represent significant or insignificant. *p < 0.05, **p < 0.01. (c) Variance partitioning analysis (VPA) of particulates, precipitates, and biofouling based on multiple linear regression.

Table 1. Range of water quality parameters

pH	Suspended solids (mg/L)	Electrical conductivity (μS/cm)	COD_{Cr} (mg/L)	BOD_5 (mg/L)	Total phosphorus (mg/L)	Total nitrogen (mg/L)	Fe^{2+} (mg/L)	Ca^{2+} (mg/L)	Mg^{2+} (mg/L)
7.3-7.8	260-410	649-823	17.8-26.8	12.7-16.4	0.81-0.93	1.27-1.64	0.28-0.35	32.8-44.7	11.7-35.9

Note: COD_{cr} represents the oxygen demand measured with potassium dichromate as the oxidant, and BOD_5 represents the oxygen consumed by oxygen-consuming microorganisms in 5 days, both of which show the degree of organic pollution of water sources.

Table 2 Parameters of drip irrigation emitters

Emitters	Rated discharge（L/h）	Geometrical parameter of flow path（mm）			Discharge coefficient	Flow index
		Length	Width	Depth		
E1	0.95	85.0	0.55	0.51	3.1	0.51
E2	2.00	24.5	0.61	0.60	6.5	0.61
E3	1.60	19.0	0.55	0.49	5.2	0.51

Physical, chemical and biological emitter clogging behaviors in drip irrigation systems using high-sediment loaded water

Yan Shen [a, b], Jaume Puig-Bargués [c], Mengyao Li [a, b], Yang Xiao [a, b *], Qiang Li [a], Yunkai Li [a, b *]

a. College of Water Resources and Civil Engineering, China Agricultural University, Beijing 100083, China

b. Engineering Research Center for Agricultural Water-Saving and Water Resources, Ministry of Education, Beijing 100083, China

c. Department of Chemical and Agricultural Engineering and Technology, University of Girona, Girona 17003, Spain

* Yang Xiao and Yunkai Li are co-corresponding authors of the article.

E-mail address: xiaoyang@cau.edu.cn (Y. Xiao); yunkai@cau.edu.cn (Y. Li)

Abstract: High-sediment water in drip irrigation (HSWDI) technology offers the opportunity to alleviate water shortages in agricultural irrigation. Emitter clogging, caused by active suspended particles, salt ions, and microorganisms present in water with high sediment load, poses considerable technical challenges to HSWDI. To date, emitter blockage of HSWDI is attributed to physical clogging, little is known about the physical, chemical, and biological clogging behaviors and their interactions for HSWDI. Here, X-ray diffraction and 16S rRNA gene sequencing were applied to determine the physicochemical minerals and microbial community structure of the foulants for HSWDI, using three types of flat emitters and two fertilization modes (no-fertigation and fertigation with ammonium polyphosphate, APP). Results indicated that HSWDI emitter clogging was not only caused by physical clogging (induced by particulates) but also caused by chemical clogging (i.e., precipitates) and biological clogging (i.e., biofilms). The main particulates in HSWDI were found to be quartz (accounting for 41.8-56.3% of total clogging foulants) and feldspar (13.6-21.1%), while the precipitates that contained calcite, dolomite and aragonite contributed 14.6-26.7%. The dominant flora in foulants were Proteobacteria (relative abundance ranged: 41.7-53.9%) and Bacteroidetes (13.6-17.3%). Moreover, the coupling effect of three types of fouling was the main reason affecting clogging (accounting for 36.3%), while the effect of two or single fouling was less (accounting for 14.4-25.3% and 0.7-2.6%). In addition, APP application caused the increase in microbial diversity and the proliferation of microorganisms, resulting in the interactions between biofilm and other two foulants (i.e., precipitates and particulates) were exacerbated, thus aggravating emitter clogging. This study opens a frontier for the investigation of physical, chemical, and biological clogging behavior, in-depth clogging mechanisms, and anti-clogging measures for HSWDI, which will facilitate the utilization of high-sediment water in agricultural irrigation.

Keywords: Composite fouling; particulate; precipitate; biofilm; ammonium polyphosphate

1 Introduction

One of the major constraints to sustainable agricultural production is a lack of irrigation water supplies (Qin et al., 2019). At present, the development of alternative water sources and the application of irrigation water-saving technologies are two key strategies to alleviate the scarcity of agricultural water resources. High-sediment Water (HSW) is widely distributed around the world, such as Northwest China, Southwest Europe, and Southeast Africa (Puertes et al., 2021; Duker et al., 2020a; Duker et al., 2020b Niu et al., 2013;), and has the potential to become an alternative water source for agricultural irrigation. Irrigation with HSW has numerous advantages, including saving conventional water resources, ensuring irrigation water consumption, and reducing irrigation costs. Meanwhile, drip irrigation is considered to be the most water-efficient irrigation technology (Nakayama and Bucks, 1991), with water-use efficiency greater than 0.9 (Wang et al., 2018a). Thus, the combination of HSW with drip irrigation technology is a viable solution to irrigation water scarcity.

The greatest barrier to the adoption and extensive use of high-sediment water drip irrigation (HSWDI) is emitter clogging, which can significantly reduce irrigation system uniformity. Currently, literature ascribes emitter clogging in HSWDI systems to physical blockage caused by suspended particle deposition (Bounoua et al., 2016; Li et al., 2019a; Niu et al., 2013). Thus, filtration has become the most common approach for controlling clogging in HSWDI. However, the control is not always satisfactory. In fact, active salt ions and microorganisms are also present in HSW (Li et al., 2019b). Even in facilities with a proper filtration system, fine particles, soluble salt ions, and microorganisms can pass through the filters and be conveyed into the emitter (Duran-Ros et al., 2009). Therefore, in addition to physical clogging, HSW irrigation may lead to chemical and biological clogging due to chemical precipitates and biofilm formation. Current research related to the clogging of HSWDI is focused on physical clogging, while chemical and biological clogging characteristics are still poorly understood.

It is noted that there may be interactions among various types of foulants (Zan et al., 2010). For instance, Umar and Saaid (2013) reported that the presence of carbonate precipitates could provide nucleation sites for

silicate particulate, thereby speeding up silicate growth. In addition, biofilm can induce calcium carbonate precipitation (Xiao et al., 2020a), which adsorbs and traps suspended particles (Zhou et al., 2016). Therefore, the relationship among various foulants may alter clogging behavior in HSWDI systems. Moreover, drip irrigation systems are used not only for irrigation, but increasingly for fertilization to improve the utilization efficiency of fertilizers and reduce soil and water pollution (Yang et al., 2011; Wang et al., 2018b). The clogging behavior in HSWDI systems may be more complicated when fertilizers are applied. Thus, this study assumed that the clogging process and interactions among various foulants would change noticeably with fertilizer application. Ammonium polyphosphate (APP) is a novel water-soluble fertilizer with high nitrogen and phosphate content, better solubility, and ease of storage. Studies have shown that phosphate fertilizers directly affect the growth of microorganisms and the production of precipitates (Muhammad et al., 2022; Xiao et al., 2020b). Moreover, it has also been demonstrated to reduce the likelihood of emitter clogging (Ma et al., 2020).

Accordingly, an in-situ experiment for assessing emitter clogging for HSWDI was conducted. The internal physical, chemical, and biological components of emitters were clarified using 16S rRNA high-throughput sequencing technology and X-ray diffraction (XRD). Three distinct types of emitters and two fertigation modes (no-fertilizer and APP application) were selected for our study. The study's aims were as follows: (1) Determine whether the emitter clogging of HSWDI contains chemical precipitation and biological fouling in addition to physical fouling? (2) If contains two or three foulants, how do they cause the emitter clogging? Such as, what is their composition? What is the relationship between foulants? (3) Clarify the impacts of APP on composite fouling in HSWDI, and provide useful practices for inhibiting clogging for HSWDI technology.

2 Material and methods

2.1 Basic operating conditions

The experimental site was located in Dengkou, Bayannaoer, Inner Mongolia Autonomous Region's North

Ulan Buhe Sand region (China). The experiment was carried out from June 2 to August 4, 2017. The experimental HSW source was Yellow River water in the Wu Shen Canal, which is a common irrigation water source in the area. Table 1 shows the Yellow River's average water quality characteristics. The concentration of suspended particles in the experimental HSW was ranged 260-410 mg/L. And the median particle size was 10.1 μm (Fig. 1a). In addition, the X-ray diffraction (XRD) pattern revealed that the dominant minerals of the suspended particles were silicate (accounting for 82.2%) and $CaCO_3$ (4.7%) (Fig. 1b). The emitter performance testing system was an independent designed platform (Fig. 2). The drip irrigation system's filter device was a combination of a sand filter (internal diameter: 101.6 mm, with filter media of particle size between 1.3 and 2.75 mm) and a disc filter (filtration level: 150 mesh). The system consisted of two sets of working devices, each stacked in four levels, with eight drip irrigation pipes of the same type arranged on each tier. The system water flow had an operating pressure of 0.1 MPa.

#Table. 1 approximately here#

#Fig. 1 approximately here#

#Fig. 2 approximately here#

Different types of emitters have different structural parameters and different hydraulic characteristics (Li et al., 2006). Particularly, the cross-sectional average velocity (v) of emitter flow channel may directly affect the mineral composition and microbial community of clogging substances. Feng et al., (2018) found that the cross-sectional average velocity could affect the speed of fouling accumulation in emitters. Meanwhile, due to the advantages of long service life and low cost, flat emitters have become a widely used type in farmland. Thus, three types of flat emitters were selected to construct different hydraulic conditions, with 30 cm spacing between emitters in this experiment. Table 2 displays the primary emitter parameters. The fertilization treatment used in this investigation was ammonium polyphosphate (APP), at 0.3 g L^{-1} (based on P_2O_5 concentration). The test had four treatments: E1, E2, E3, and E3.APP. In previous studies, the different content of clogging substances was

found in different type emitters, but the types of clogging substances did not show significant differences (Li et al., 2019b), so only one type of emitter (E3) was selected for APP application. The system employed an accelerated method to run once per day (Han et al., 2019), which was equivalent to the actual irrigation or fertilization in the farmland once. The system ran for 10h every day (8:00-18:00), accumulatively for 64 days. The flow rate of the emitters was 0.375 m^3 d^{-1}, and the fertilizer rate was 25 g d^{-1}. The system used the Yellow River water-fertilization water-Yellow River water alternate operation, with fertilization occurring near the middle of the total running time recorded by the company (supplementary materials, Table S1) (Li et al., 2007). To flush the drip irrigation pipe, the system activated the tail flushing valve every 64 h. The flushing velocity was set to 0.40 m s^{-1} and the flushing time was set to five min by regulating the system pressure.

#Table. 2 approximately here#

2.2 The performance evaluation index of emitters

Emitter performance was assessed using the average discharge variation rate (Dra) and the Christiansen coefficient of uniformity (CU).

The emitters' average discharge variation rate can be expressed by formula (1) (Zhou et al., 2015).

$$Dra = \frac{\sum_{i=1}^{n} \frac{q_i^t}{q_i^0}}{n} \times 100\% \quad (1)$$

Where q_i^0 represents the starting flow rate of the emitter i, in L h^{-1}; q_i^t represents the flow rate of the emitter i at t days, in L h^{-1}; n represents the number of all emitters along a drip irrigation pipe.

The emitters' Christiansen coefficient of uniformity can be expressed by formula (2) (Christiansen, 1942).

$$CU = 100\left(1 - \frac{\sum_{i=1}^{n} |q_i^t - \bar{q}^t|}{n\bar{q}^t}\right) \quad (2)$$

Where $\bar{q}^t$ represents the average flow rate of all emitters along the drip irrigation pipe at t time, in L h^{-1}.

2.3 Extraction and treatment of emitter clogging content

2.3.1 Extraction of clogging substances

Every eight days, the dry weight (DW) of clogging substances was measured from five emitters which were randomly chosen at the head (emitters 1-30), middle (31-60), and tail (61-90) of each drip irrigation tape. There were three repeatability tests in one sampling process. Three drip irrigation laterals were arranged for one treatment in a sampling, and were removed from the experiment system after sampling. The 15 emitter samples were mixed and dried at 60 °C for 20 minutes. The dried emitters and those containing foulants were weighed. The clogging substances in emitter samples were washed using an ultrasonic cleaner (frequency: 100 Hz), and the washed emitters were dried and weighed. DW was calculated using the weight differential.

2.3.2 The mineral makeup and morphology analysis of fouling in emitters

Mineral composition of fouling was tested every 16 days. The clogging substance suspension (previously separated in the dry weight test) was centrifuged at 4000 rpm. The supernatant was discarded after centrifugation to collect the bottom solid phase. To obtain dry weight of clogging substances, the bottom solid phase material was oven-dried. Mineral makeup was determined using an X-ray diffractometer (brand: Bruker, Germany; work conditions were: 40 kV voltage, 40 mA current, Cu target, and 1.5406 Å wavelength). The surface morphology of the fouling in emitters at the end of the experiment was observed using a scanning electron microscope (SEM). The specific operation steps are as follows: the sample is fixed on the sample stage by a conductive tape, and is placed in a vacuum chamber to spray the conductive gold film before scanning. Machine conditions were: acceleration voltage 30kV, magnification 2000×.

2.3.3 16S rRNA-based microbial community analysis

Genomic DNA extraction from samples was by sodium dodecyl sulfate (SDS) method. The purity and concentration of DNA were checked using agarose gel electrophoresis. Ultrapure water was added to dilute the resulting genomic DNA to 1 ng L^{-1}. Diluted genomic DNA serves as a template. Barcode's specific primers and enzymes (Manufacturer: New England Biolabs; Product name: Phusion® High-Fidelity PCR Master Mix with GC Buffer) were applied for PCR amplification. After detection and purification of PCR products, a library kit (brand:

Thermo Fisher) was used for gene library construction. After the test was qualified, the PCR products of the sample were subjected to high-throughput sequencing on the IonS5^{TM}XL platform (DNA sequencing system; Manufacturer: Thermo Fisher Scientific). The obtained data were filtered by Cutadapt software for species classification analysis of Operational Taxonomic Units (OTUs). Species annotation and abundance assessment were performed for each OTUs based on the analysis results. Qiime software (Version 1.9.1) was used to analyze the microbial diversity index (Ace and Chao, the higher the index, the more abundant the flora) in the sample.

2.4 Statistical analysis

The significant changes in mineral content among the four treatments (E1, E2, E3, and E3.APP) were analyzed by paired t-test. The difference in microbial diversity index across groups was analyzed using the Wilcoxon rank-sum test. The differences in microbial community structure across different treatments were determined using similarity analysis (ANOSIM). Linear discriminant analysis effect size (LDA effect size, LEFSe) was chosen to assess and identify species (biomarkers) that varied significantly between treatments. The differences in the microbial communities were illustrated by non-metric multidimensional scaling (NMDS). Structural equation modeling analysis (SEMA) was applied to describe the interaction between fouling, and the effect on system clogging. Variance partitioning analysis (VPA) was employed to describe the contribution of single fouling and coupling between fouling to system clogging. Spearman analysis was performed to evaluate the correlation between the clogging parameters of the emitters (Dra, CU, DW, and various mineral components) and the different species. $p < 0.05$ was the maximum level in the significance analysis.

3 Results

3.1 Emitter performance and clogging substances content in HSWDI

The emitters' average discharge variation rate (Dra) and Christiansen coefficient of uniformity (CU) representing the emitter performance level both exhibited a gradual drop from 0-32 days and a fast decline from

32-64 days (Fig. 3). Different descending speed may be related to the accumulation law of the clogging substances in emitters. There were some differences in Dra and CU between different emitter treatments. The E2 emitter showed higher Dra and CU and therefore was less prone to clogging. Compared with E2, the Dra in E1 and E3 emitters were decreased by 1.5-14.7% and 0.9-3.7%, respectively, while the CU in E1 and E3 emitters was decreased by 1.3-17.1% and 0.8-9.9%. When APP was used as fertilizer, clogging was exacerbated. APP reduced Dra and CU by 0.8-19.1% and 2.0-21.4%, respectively, when compared to E3.

The clogging substance dry weight (DW) results demonstrated a gradual increase at first, then, after 40 days, they had a quick upward trend. Similar, to the results of Dra and CU, the DW of the E2 emitter was the lowest. The DW of E1 and E3 emitters increased by 21.6-83.6% and 6.7-19.6%, respectively, as contrasted to E2. APP accelerated the accumulation of DW, increasing by 42.2-123.1% the DW of emitter clogging substances in E3.APP as compared to E3. Scanning electron microscope (SEM) shows the real morphology of fouling at the end of the experiment (Fig. 4). Different types of fouling were intertwined, indicating that there were more than just particulates in the HSWDI emitter clogging substances.

#Fig. 3 approximately here#

#Fig. 4 approximately here#

3.2 Influence of HSWDI on particulates and precipitates in the emitters.

The mineral composition information of particulates and precipitates found inside emitters are shown in Fig. 5. Calcite, dolomite, aragonite, feldspar, muscovite, chlorite, and quartz were determined to be the most common minerals found inside emitters. Calcite, feldspar, and quartz make up the bulk of emitters clogging substances, contributing 5.8-16.6%, 13.6-21.1%, and 41.8-56.3% of total clogging content, respectively. Particulates (quartz, feldspar, muscovite, chlorite) and precipitates (calcite, dolomite, aragonite) were responsible for 73.3-85.4% and 14.6-26.7%. of the total. There was no significant difference in the mineral ratio of the three emitters without fertilization. Mineral proportions were altered when APP was applied, APP increased the calcite and dolomite

levels in precipitates. In comparison to E3, the relative quantities of calcite and dolomite in E3.APP increased by 4.3% -5.8% and 0.6-3.0%, respectively. Quartz decreased by 4.9-12.0% as a relative proportion of APP.

#Fig. 5 approximately here#

The contents of particulates and precipitates (Fig. 6) were 16.3-20.2 mg cm^{-2} and 5.2-9.3 mg cm^{-2}, respectively, when system operation ended. Results showed that quartz was the most abundant in the three emitter treatments (E1, E2, E3), and E1 had the greatest number of particulates and precipitates. Compared with E3, the content of particulates and precipitates rose considerably after the APP treatment ($p < 0.05$, Table S2 in supplementary materials). The concentrations of particulates and precipitates in the E3.APP treatment increased by 0.4-2.6 mg cm^{-2} and 0.6-3.7 mg cm^{-2}. The content of precipitates in the E3.APP was considerably higher than other treatments. Among the three minerals representing precipitates (calcite, dolomite and aragonite) in Fig. 6, rapid accumulation of calcite (increase 0.3-1.9 mg cm^{-2} compared to three treatments without ammonium polyphosphate) may be the main reason for this result.

#Fig. 6 approximately here#

3.3 Microbial community diversities and intergroup difference analysis

Fig. 7a and 7b depict the differences in the diversity indices (i.e., Ace and Chao). Microbial diversity for foulants of E2 and E1 emitter were always the lowest and the highest, respectively, throughout the experiment. The other two diversity indexes are shown in supplementary materials (Fig. S1). The microbial community's diversity was significantly ($p < 0.05$) boosted by APP (supplementary materials, Table S4). Fig. 7d shows the taxonomic dendrogram of the detected bacterial communities (taxonomic dendrogram of E3.APP is shown in the Fig. S2 of supplementary materials). After the samples were subjected to 16S rRNA gene sequencing, a total of 933,492 clean reads and 2243 OTUs were detected. Only a few OTUs (33-129) had significant differences in relative abundance between E1, E2 and E3, while most OTUs did not show significant statistical differences. The different OTUs were mainly found between Proteobacteria, Bacteroides, and Acidobacteria. The microbial

community structure at the phylum level (top10) and the clustering abundance information of species at the genus level (top35) are shown in Fig 7c and Fig 7e. The relative abundances of Proteobacteria and Bacteroides were higher in the three treatments without fertilization, being 41.7-53.9% and 13.6-17.3%, respectively. These two types of bacteria accounted for more than 68.5% of the total species. The different types of emitters (E1, E2, and E3) showed relatively minor changes in genus-level species, and the abundance variation area was focused between top14 and top21 (*Streptococcus-Rheinhermera*). Bacteroides relative abundance increased by 22.4% after applying APP but, conversely, Proteobacteria relative abundance declined by 14.9%. The species abundance heatmap revealed that APP had a considerable impact on microbial community structure. APP increased the abundance of 13 main species (top1-top13, *Terrimonas-Cytophaga*) while reducing the proportion of some species (top22-top35, *Sphingomonas-llumatobacter*).

#Fig. 7 approximately here#

To identify bacterial taxa with significant differences between different treatments, LDA effect size (LEFSe) analysis (cladogram and LDA histogram) and non-metric multidimensional scaling (NMDS) were used to classify biomarkers (Fig. 8). Proteobacteria and Bacteroides were the most important microbial communities in different treatments, according to the cladogram (Fig. 8a). LDA histogram (Fig. 8b) depicted 19 significantly different species. E1, E2, E3, and E3.APP had seven, three, two, and seven significantly different species, respectively. The NMDS clearly reflected differences between and within different treatment groups. Sample points of different emitters were relatively close, with E3.APP being far away from the E1, E2, and E3 sample points after fertilization, indicating that the difference in microbial community structure between different emitters was relatively minor ($p < 0.05$, Fig. S3 in supplementary materials).

#Fig. 8 approximately here#

3.4 Interactions and clogging contribution of composite fouling

The link between biofouling, particles, and precipitates was demonstrated by Spearman analysis (Fig. 9a).

Dra and CU exhibited a significant negative relationship with the diversity index, while DW had a highly significant positive relationship ($p < 0.01$, Table S5 in supplementary materials). Particulates/precipitates and microbiological diversity had little positive connection, whereas calcite in precipitates had a highly significant positive association ($p < 0.01$, Table S5 in supplementary materials). Almost all bacteria had a positive or negative correlation with certain indicators.

Fig. 9b shows the relationship between fouling and emitter clogging, while Fig. 9c reveals the contribution of fouling to clogging. Precipitates and particulates were found in significant correlation with DW ($\gamma = 0.828$, $p < 0.01$; $\gamma = 0.453$, $p < 0.05$), accelerating emitter clogging by directly affecting DW. Biofouling had a weak negative effect on DW ($\gamma = -0.105$, $p < 0.01$). However, biofouling and precipitates, as well as biofouling and particulates, had a strong relationship with clogging ($\gamma = 0.771$, $p < 0.01$; $\gamma = 0.413$, $p < 0.05$). Biological fouling promoted the formation of chemical precipitation and particle precipitation to reduce the Dra and CU of the emitters. For the result of variance partitioning analysis (VPA), particulates, precipitates, and biofouling alone contributed little to the formation of total dry weight, but the three together contributed 36.3% to the formation of total dry weight. Among them, particulates and precipitates, and biofouling and precipitates contributed 25.3% and 14.4%, respectively, to the formation of total dry weight of clogging substances.

#Fig. 9 approximately here#

4 Discussion

4.1 Clogging of high-sediment water drip irrigation was not caused by physical clogging alone

Clogging caused by high-sediment loaded water in the drip irrigation system is often attributed to deposition of particulates (Bove et al., 2017; Duran-Ros et al., 2009a). In this study, in addition to particulates a large number of precipitates (i.e., calcite, muscovite, and aragonite) were found in HSWDI, contributing to more than 25% of clogging substances. Moreover, a great number of different microorganisms were found present in the clogging

substances by 16S rRNA sequencing technology and further contributed to composite fouling of emitters. Zhou et al. (2019) reported that the microbial content in high sediment water was 2-3 times that in reclaimed effluents. Moreover, numerous ions were present in the high sediment water, easily interacting to produce a precipitate (Li et al., 2019b). It was found the water source particles were mainly silicate (82.2%) with only a small amount of calcite precipitation (4.7%, Fig. 1b). While the precipitates (calcite, dolomite and aragonite) accounted for 14.6-26.7% of the total clogging substances, indicating the deposition of suspended solids in the water source contributed less to the formation of precipitates. In fact, massive accumulation of precipitates often occurs after the drip irrigation system has finished irrigation. After the undischarged water is evaporated by sunlight, the crystallization caused by the saturation of the internal salt is the main factor for the formation of the precipitates. Thus, the clogging problem of HSWDI emitters in this study can not be simply attributed to the physical clogging caused by conventional particulates. Mineral-induced chemical clogging and biological fouling caused by microorganisms must both be considered.

In fact, the different types of fouling identified did not act independently in HSWDI. Only less than 5% of the contribution to the decline of the system Dra could be explained by single fouling, however the contribution of three types of fouling coupling were 36.3%. Almost all biomarkers were related to precipitates or particulates (Fig. 9a), and interactions were evidenced among particulates, precipitates, and biofouling (Fig. 9b and Fig. 9c). The physical-chemical (particulates-precipitates) interaction contributed 25.3% to system clogging. Lioliou et al. (2007) indicated that silicate could reduce the time for carbonate to induce nucleation by reducing surface energy . Meanwhile, the generated calcium carbonate might absorb silicon ions on the crystal surface, culminating in a combination of silicate and carbonate solids (John et al., 2018; Garrault-Gauffinet and Nonat, 1999). The biological-chemical (biofouling-precipitates) interaction contributed 14.4% to system blockage in this study. Several researches had proven that bacteria could generate biological macromolecules through metabolic processes and deposited inorganic ions in the surrounding environment (Guo et al., 2020; Pasquale et al., 2019;

Song et al., 2019; Wang et al., 2020). In addition, microorganisms could also promote the deposition of carbonates by increasing the CO_3^{2-} content in the solution and lowering the pH of the surrounding environment (Schwantes-Cezario et al., 2017; Zheng, 2021). This phenomenon demonstrates that HSWDI blockage is frequently the consequence of two or three types of fouling and that no one form of fouling has a dominant role.

4.2 The effects of APP on emitter clogging in HSWDI system

There were some differences in the relative content proportions of fouling, microbial diversity indexes, and community structure abundance in the three types of emitters selected in the experiment ($p < 0.05$, Fig. S3 in supplementary materials). This indicated that different hydraulic conditions will influence on the particle, precipitates and microbial conditions in emitters. APP altered the microbial community structure present in the E3 emitter, greatly promoting the deposition of particulates and precipitates. With regard to biofouling, APP increased microorganism growth, resulting in an increase in the microbial diversity index. Increase diversity might be connected to the high levels of nitrogen and phosphorus in APP since nitrogen and phosphorus play a major role in microbial metabolism, supporting bacterial proliferation (Lu et al., 2016; Wu et al., 2018). Under APP application, additional biomarkers were discovered. Biofouling, on the other hand, had a highly significant positive association with the overall quantity of clogging substances in the structural equation modeling analysis (SEMA, $p < 0.01$). The correlation of biofouling with clogging suggests that the newly created biomarkers likely speed up the development of precipitates and particulates, leading to a cascade of biomineralization processes that clog emitters (Chen et al., 2019; Gong et al., 2009; Thompson et al., 2012).

Compared with precipitates in the E3 emitter, the application of APP (the corresponding treatment is E3.APP) resulted in a 60.6-185.8% rise in this study. However, Ma et al. (2020) discovered that APP lowered carbonate levels in drip irrigation systems. However, similar results were not observed in the present study. The variation in microbiological conditions between the two different studies could cause this difference. The water source used by Ma et al. (2020) was a high salinity water. Consequently high concentration of salt ions hindered the growth of

bacteria, resulting in decreased microbial levels, thus the application of APP would not cause a large number of microbes to multiply (Fu et al., 2019; Liu et al., 2019). Besides biological factors, APP itself developed a chain structure after a breakdown. The chelating ability of chain phosphates on calcium ions was weaker than that of magnesium and iron ions, making it easier to disperse calcium ions in the solution, and carbonate ions were easier to capture surrounding calcium ions (Rashchi et al., 2000; Van Wazer and Callis, 1958).

Although the increase in particulate content was less than the rise in carbonate content, APP did produce an 8.6-39.5% increase in particulate content. The flocculation of microorganisms and their metabolites, capturing suspended particles in the surrounding environment, seemed the more likely source of this phenomenon (Wang et al., 2014; Zhang et al., 2020).

4.3 Practical application method of HSWDI drip irrigation technology

Particulates are currently considered to be the most direct cause of clogging in HSWDI. However, this investigation discovered that clogging compounds contained a noticeable number of precipitates and biofouling. Thus, in the application of high sediment water, biofouling and precipitates also need to be considered to controll the performance of drip irrigation systems.

Microorganisms that act as accelerators of both precipitates and particulates should be prioritized for removal to better regulate precipitates and particulates in emitters. Targeted microbial control measures are the key to reducing the adhesion and growth of microorganisms in emitters. The hypochlorous acid formed by chlorine in contact with water has strong oxidizing properties, so it is often used to kill water-borne pathogens. Chlorine is regularly added to drip irrigation systems to reduce the activity of the flora, or even inactivate, thereby controlling the colonization and growth of microorganisms (Pressman et al., 2012). However, chlorination can result in negative issues such as soil contamination, agricultural yield decrease, and water pollution. Recently, an eco-friendly method using microbial antagonism technology has gained increasing interest for controlling emitter biofouling. By secreting bactericidal chemicals that vie for space and nutrition, exogenous bacteria can suppress

or even kill existing germs. Wen et al. (2021) discovered that *Bacillus amyloliquefaciens* could prevent biofouling in drip irrigation systems by generating a range of antibiotics. This bacterial treatment is a possible biofouling control approach for the HSWDI system.

Carbonate was regarded as a typical chemical fouling contributor in HSWDI systems. The conventional method of control is to add acid regularly to the drip irrigation system (Kreij et al., 2003; Yuan et al., 1998). However, Similar to chlorination, acidification also brings environmental risks. Reducing the concentration of salt segregants in the water source was found to be the most effective way to alleviate carbonate precipitation in HSW. Water softeners effectively reduce precipitation of carbonate and inhibit scale (Brastad and He, 2013). Water softeners, on the other hand, pollute irrigation water by injecting distinctive kinds of ions. For this reason, dosage should be monitored through use, and content of introduced ions.

Filters are widely utilized in agriculture due to the high amount of quartz and silicate in high-sediment water. However, despite the presence of a competent multi-stage filtering system (i.e., sand filter and disc filter) in this test system, the HSWDI system still contained a significant quantity of quartz and silicate. This is due to the fact that the filtration system had an effective filtering on coarse particles, but a poor filtering ability on fine particles (Li et al., 2021; Liu et al., 2021). Thus, fine particles may directly enter the system through filter pores. Current filter designs frequently allow more fine particles to pass to obtain maximum economic benefit, extending filtering cycles or lowering the number of backwashes to minimize energy consumption (Hou et al., 2022). However, fine particles can also exacerbate the clogging of drip irrigation systems. Particle size distribution of the high-sediment water used in this study is similar to the normal distribution with x = 10 as the central axis. As a result, we recommend that the filter filtration level should be greater than 10 μm (1340 mesh) when choosing a filtration system for HSWDI, and the filtering efficiency of fine particles should be prioritized over energy consumption.

5 Conclusions

(1) High-sediment water drip irrigation (HSWDI) emitter clogging was not only caused by physical clogging. Particulates, precipitates, and biofouling were discovered in the clogging substances.

(2) Quartz, feldspar and calcite had the largest proportions in the clogging substances, accounting for 41.8-56.3%, 13.6-21.1% and 5.8-16.6% of clogging substances, respectively. At the level of the phylum in biological fouling, Proteobacteria, Bacteroidetes, and Acidobacteria were predominant accounting for 41.7-53.9%, 13.6-17.3%, and 8.9-13.8%, respectively.

(3) Particulates, precipitates, and biofouling had an obvious mutual promotion effect. the coupling of three fouling was the main reason affecting clogging (accounting for 36.3%), while the effect of two or single fouling was less (accounting for 14.4-25.3% and 0.7-2.6%).

(4) Ammonium polyphosphate (APP) increased the generation of precipitates and particulates and affected the microbial diversity and community structure dramatically. The precipitates and particulates caused by APP increased by 60.6-185.8% and 8.6-39.5%, respectively, over no APP (E3 and E3.APP, a same emitter type without or with APP). The different species produced after the application of APP were mainly Bacteroidetes, Sphingobacteriales, Saccharibacteria, Terrimonas, and Betaproteobacteria.

Acknowledgements

Funding support for this research is provided by National Natural Science Foundation of China (51790531, 51621061).

References

Bounoua, S., Tomas, S., Labille, J., Molle, B., Granier, J., Haldenwang, P., Izzati, S.N., 2016. Understanding physical clogging in drip irrigation: in situ, in-lab and numerical approaches. Irrig. Sci. 34, 327-342. https://doi.org/10.1007/s00271-016-0506-8

Bove, J., Puig-Bargues, J., Arbat, G., Duran-Ros, M., Pujol, T., Pujol, J., Ramirez de Cartagena, F., 2017.

Development of a new underdrain for improving the efficiency of microirrigation sand media filters. Agric. Water Manage. 179, 296-305. 296-305. https://doi.org/10.1016/j.agwat.2016.06.031

Brastad, K.S., He, Z., 2013. Water softening using microbial desalination cell technology. Desalination 309, 32-37. https://doi.org/10.1016/j.desal.2012.09.015

Chen, L., Redmile-Gordon, M., Li, J., Zhang, J., Xin, X., Zhang, C., Ma, D., Zhou, Y., 2019. Linking cropland ecosystem services to microbiome taxonomic composition and functional composition in a sandy loam soil with 28-year organic and inorganic fertilizer regimes. Appl. Soil Ecol. 139, 1-9. https://doi.org/10.1016/j.apsoil.2019.03.011

Christiansen, J.E., 1942. Irrigation by sprinkling. Calif. Agr. 670, 1-124.

Duker, A., Cambaza, C., Saveca, P., Ponguane, S., Mawoyo, T.A., Hulshof, M., Nkomo, L., Hussey, S., Van der Pol, B., Vuik, R., Sitgter, T., van der Zaag, P., 2020a. Using nature-based water storage for smallholder irrigated agriculture in African drylands: Lessons from frugal innovation pilots in Mozambique and Zimbabwe. Environ. Sci. Policy 107, 1-6. https://doi.org/10.1016/j.envsci.2020.02.010

Duker, A.E.C., Mawoyo, T.A., Bolding, A., Fraiture, C.D., Zaag, P.V.D., 2020. Shifting or drifting? The crisis-driven advancement and failure of private smallholder irrigation from sand river aquifers in southern arid Zimbabwe. Agric. Water Manage. 241, 106342. https://doi.org/10.1016/j.agwat.2020.106342

Duran-Ros, M., Puig-Bargués, J., Arbat, G., Barragán, J., Cartagena, F., 2009a. Effect of filter, emitter and location on clogging when using effluents. Agric. Water Manage. 96, 67-79. https://doi.org/10.1016/j.agwat.2008.06.005

Feng, J., Y. K. Li., Z. Y. Liu., T. Muhammad and R. N. Wu., 2019. Composite clogging characteristics of emitters in drip irrigation systems. Irrig. Sci. 37(2). 105-122. doi: 10.1007/s00271-018-0605-9

Fu, G., Zhao, L., Huangshen, L., Wu, J., 2019. Isolation and identification of a salt-tolerant aerobic denitrifying bacterial strain and its application to saline wastewater treatment in constructed wetlands. Bioresource Technol. 290, 121725. https://doi.org/10.1016/j.biortech.2019.121725

Garrault-Gauffinet, S., Nonat, A., 1999. Experimental investigation of calcium silicate hydrate (C-S-H) nucleation. J. Cryst. Growth 200, 565-574. https://doi.org/10.1016/S0022-0248(99)00051-2

Gong, W., Yan, X., Wang, J., Hu, T., Gong, Y., 2009. Long-term manure and fertilizer effects on soil organic matter fractions and microbes under a wheat-maize cropping system in northern China. Geoderma 149, 318-324. https://doi.org/10.1016/j.geoderma.2008.12.010

Guo, N., Wang, Y., Hui, X., Zhao, Q., Liu, T., 2020. Marine bacteria inhibit corrosion of steel via synergistic biomineralization. J. Mater. Sci. Technol. 66, 82-90. https://doi.org/10.1016/j.jmst.2020.03.089

Han, S., Li, Y., Zhou, B., Liu, Z., Feng, J., Xiao, Y., 2019. An in-situ accelerated experimental testing method for drip

irrigation emitter clogging with inferior water. Agric. Water Manage. 212, 136-154. https://doi.org/10.1016/j.agwat.2018.08.024

Hou, P., Puig-Bargués, J., Xiao, Y., Xue, T., Wang, J., Song, P., Li, Y., 2022. A Novel Improved Method of Centrifugal Filter for Separating Water and Fine Sediment: Appropriately Increase Energy Consumption for High Efficiency. Irrig. Sci. 40 (2), 151-161. https://doi.org/10.1007/s00271-021-00765-9

John, E., Matschei, T., Stephan, D., 2018. Nucleation seeding with calcium silicate hydrate – A review. Cement Concrete Res. 113, 74-85. https://doi.org/10.1016/j.cemconres.2018.07.003

Kreij, C.D., Burg, A.M.M.V.D., Runia, W.T., 2003. Drip irrigation emitter clogging in Dutch greenhouses as affected by methane and organic acids. Agric. Water Manage. 60, 73-85. https://doi.org/10.1016/S0378-3774(02)00159-2

Li, J., Meng, Y., Li, B., 2007. Field evaluation of fertigation uniformity as affected by injector type and manufacturing variability of emitters. Irrig. Sci. 25 (2), 117-125. https://doi.org/10.1007/s00271-006-0039-7

Li, Q., Song, P., Zhou, B., Xiao, Y., Muhammad, T., Liu, Z., Zhou, H., Li, Y., 2019a. Mechanism of intermittent fluctuated water pressure on emitter clogging substances formation in drip irrigation system utilizing high sediment water. Agric. Water Manage. 215, 16-24. https://doi.org/10.1016/j.agwat.2019.01.010

Li, Y., Chen, Y., Xia, W., Xie, G., 2021. Filtration of kaolinite and coal mixture suspension: Settling behavior and filter cake structure analysis. Powder Technol. 381, 122-128. https://doi.org/10.1016/j.powtec.2020.12.050

Li, Y., Pan, J., Chen, X., Xue, S., Feng, J., Muhammad, T., Zhou, B., 2019b. Dynamic effects of chemical precipitates on drip irrigation system clogging using water with high sediment and salt loads. Agric. Water Manage. 213, 833-842. https://doi.org/10.1016/j.agwat.2018.11.021

Li Y., Pei Y., Shu R., Ting X., 2006. Hydraulic characterizations of tortuous flow in path drip irrigation emitter. J. Hydrodyn 18: 449-457. https://doi.org/10.1016/j.jcis.2006.12.045

Lioliou, M.G., Paraskeva, C.A., Koutsoukos, P.G., Payatakes, A.C., 2007. Heterogeneous nucleation and growth of calcium carbonate on calcite and quartz. J. Colloid Interf. Sci. 308, 421-428. https://doi.org/10.1016/j.jcis.2006.12.045

Liu, F.-f., Fan, J., Du, J., Shi, X., Zhang, J., Shen, Y., 2019. Intensified nitrogen transformation in intermittently aerated constructed wetlands: Removal pathways and microbial response mechanism. Sci. Total Environ. 650, 2880-2887. https://doi.org/10.1016/j.scitotenv.2018.10.037

Liu, Z., Muhammad, T., Puig-Bargues, J., Han, S., Ma, Y., Li, Y., 2021. Horizontal roughing filter for reducing emitter composite clogging in drip irrigation systems using high sediment water. Agric. Water Manage. 258. https://doi.org/10.1016/j.agwat.2021.107215

Lu, H., Feng, Y., Wu, Y., Yang, L., Shao, H., 2016. Phototrophic periphyton techniques combine phosphorous removal

and recovery for sustainable salt-soil zone. Sci. Total Environ. 568, 838-844. https://doi.org/10.1016/j.scitotenv.2016.06.010

Ma, C., Xiao , Y.., .Puig-Bargués, J., Shukla, M.K., Tang, X., Hou, P., Li, Y., 2020. Using phosphate fertilizer to reduce emitter clogging of drip fertigation systems with high salinity water. J. Environ. Manage. 263, 110366. https://doi.org/10.1016/j.jenvman.2020.110366

Muhammad, T., Li, L., Xiao, Y., Zhou, Y., Liu, Z., He, X., Bazai, N.A., Li, Y., 2022. Multiple fouling dynamics, interactions and synergistic effects in brackish surface water distribution systems. Chemosphere 287. https://doi.org/10.1016/j.chemosphere.2021.132268

Nakayama, F.S., Bucks, D.A., 1991. Water quality in drip/trickle irrigation: A review. Irrig. Sci. 12, 187-192. https://doi.org/10.1007/BF00190522

Niu, W., Liu, L., Chen, X., 2013. Influence of fine particle size and concentration on the clogging of labyrinth emitters. Irrig. Sci 31 (2), 545-555. https://doi.org/10.1007/s00271-012-0328-2

Pasquale, V., Fiore, S., Hlayem, D., Lettino, A., Huertas, F.J., Chianese, E., Dumontet, S., 2019. Biomineralization of carbonates induced by the fungi Paecilomyces inflatus and Plectosphaerella cucumerina. Int. Biodeter. Biodegr. 140, 57-66. https://doi.org/10.1016/j.ibiod.2019.03.005

Pressman, J.G., Lee, W.H., Bishop, P.L., Wahman, D.G., 2012. Effect of free ammonia concentration on monochloramine penetration within a nitrifying biofilm and its effect on activity, viability, and recovery. Water Res. 46 (3), 882-894. https://doi.org/ 10.1016/j.watres.2011.11.071

Puertes, C., Bautista, C., Lidón, A., Francés, F., 2021. Best management practices scenario analysis to reduce agricultural nitrogen loads and sediment yield to the semiarid Mar Menor coastal lagoon (Spain). Agr. Syst. 188. https://doi.org/10.1016/j.agsy.2020.103029

Qin, Y., Mueller, N.D., Siebert, S., Jackson, R.B., Davis, S.J., 2019. Flexibility and intensity of global water use. Nat. Sustain. 2, 515-523. https://doi.org/10.1038/s41893-019-0294-2

Rashchi, F., Finch, J.A. 2000. Polyphosphates: A review their chemistry and application with particular reference to mineral processing. Miner. Eng. 13, 1019-1035. https://doi.org/10.1016/S0892-6875(00)00087-X

Schwantes-Cezario, N., Medeiros, L.P., Oliveira, A.D., Nakazato, G., Renata, K., Toralles, B.M., 2017. Bioprecipitation of calcium carbonate induced by Bacillus subtilis isolated in Brazil. Int. Biodeter. Biodeg. 123, 200-205. https://doi.org/10.1016/j.ibiod.2017.06.021

Song, J., Han, B., Song, H., Yang, J., Zhang, L., Ning, P., Lin, Z., 2019. Nonreductive biomineralization of uranium by Bacillus subtilis ATCC-6633 under aerobic conditions. J. Environ. Radioactiv. 208-209, 106027. https://doi.org/10.1016/j.jenvrad.2019.106027

Thompson, J., Lin, N., Lyster, E., Arbel, R., Knoell, T., Gilron, J., Cohen, Y., 2012. RO membrane mineral scaling in the presence of a biofilm. J. Membrane Sci. 415, 181-191. https://doi.org/ 10.1016/j.memsci.2012.04.051

Umar, A.A., Saaid, I.B.M., 2013. Silicate Scales Formation During ASP Flooding: A Review. Research J. Appl. Sci. Eng. Technol. 6, 1543-1555. https://doi.org/ 10.19026/rjaset.6.3867

Van Wazer, J., Callis, C., 1958. Metal Complexing by Phosphates. Chem. Rev. 58 (6), 1011-1046. https://doi.org/10.1021/cr50024a001

Wang, B.-B., Peng, D.-C., Hou, Y.-P., Li, H.-J., Pei, L.-Y., Yu, L.-F., 2014. The important implications of particulate substrate in determining the physicochemical characteristics of extracellular polymeric substances (EPS) in activated sludge. Water Res. 58, 1-8. https://doi.org/10.1016/j.watres.2014.03.060

Wang, H., Wu, L., Cheng, M., Fan, J., Zhang, F., Zou, Y., Chau, H.W., Gao, Z., Wang, X., 2018a. Coupling effects of water and fertilizer on yield, water and fertilizer use efficiency of drip-fertigated cotton in northern Xinjiang, China. Field Crop. Res. 219, 169-179. https://doi.org/ 10.1016/j.fcr.2018.02.002

Wang, J., Niu, W., Guo, L., Liu, L., Li, Y., Dyck, M., 2018b. Drip irrigation with film mulch improves soil alkaline phosphatase and phosphorus uptake. Agric. Water Manage. 258-267. https://doi.org/ 10.1016/j.agwat.2017.12.022

Wang, X., Jiang, H., Zheng, G., Liang, J., Zhou, L., 2020. Recovering iron and sulfate in the form of mineral from acid mine drainage by a bacteria-driven cyclic biomineralization system. Chemosphere 262, 127567. https://doi.org/10.1016/j.chemosphere.2020.127567

Wen, J., Xiao, Y., Song, P., Sun, B., Muhammad, T., Ma, L., Aosiman, A.W., Li, Y., 2021. Bacillus amyloliquefaciens application to prevent biofilms in reclaimed water microirrigation systems. Irrig. Drain. 70, 4-15. https://doi.org/ 10.1002/ird.2527

Wu, Y., Liu, J., Rene, E.R., 2018. Periphytic biofilms: A promising nutrient utilization regulator in wetlands. Bioresource Technol. 248, 44-48. https://doi.org/10.1016/j.biortech.2017.07.081

Xiao, Y., Jiang, S.C., Wang, X., Muhammad, T., Song, P., Zhou, B., Zhou, Y., Li, Y., 2020a. Mitigation of biofouling in agricultural water distribution systems with nanobubbles. Environ. Int. 141, 105787. https://doi.org/10.1016/j.envint.2020.105787

Xiao, Y., Puig-Bargués, J., Zhou, B., Li, Q., Li, Y., 2020b. Increasing phosphorus availability by reducing clogging in drip fertigation systems. J. Clean. Prod. 262. https:/doi.org/10.1002/ird.2527

Yang, L.J., Zhang, Y.L., Li, F.S., Lemcoff, J.H., 2011. Soil Phosphorus Distribution as Affected by Irrigation Methods in Plastic Film House. Pedosphere 21, 712-718. https://doi.org/10.1016/S1002-0160(11)60174-4

Yuan, Z., Waller, P.M., Choi, C.Y., 1998. Effects of organic acids on salt precipitation in drip emitters and soil. T. ASAE 41 (6), 1689-1696. https://doi.org/ 10.13031/2013.17345

Zan, C., Shi, L., Xiujuan, M.A., Yang, W., 2010. Evolution of composite fouling on a vertical stainless steel surface caused by treated sewage. Front. Energy 4 (2), 171-180. https://doi.org/ 10.1007/s11708-009-0068-z

Zhang, W., Niu, W., Li, G., Wang, J., Wang, Y., Dong, A., 2020. Lateral inner environment changes and effects on emitter clogging risk for different irrigation times. Agric. Water Manage. 233, 106069. https://doi.org/10.1016/j.agwat.2020.106069

Zheng, T., 2021. Bacteria-induced facile biotic calcium carbonate precipitation. J. Cryst. Growth 563 (2), 126096. https://doi.org/ 10.1016/j.jcrysgro.2021.126096

Zhou, B., Li, Y., Liu, Y., Xu, F., Pei, Y., Wang, Z., 2015. Effect of drip irrigation frequency on emitter clogging using reclaimed water. Irrig. Sci. 33, 221-234. https://doi.org/10.1007/s00271-015-0461-9

Zhou, B., Li, Y., Xue, S., Feng, J., 2019. Variation of microorganisms in drip irrigation systems using high-sand surface water. Agric. Water Manage. 218, 37-47. https://doi.org/10.1016/j.agwat.2019.02.038

Zhou, B., Li, Y.K., Song, P., Xu, Z.C., Bralts, V., 2016. A kinetic model for biofilm growth inside non-PC emitters under reclaimed water drip irrigation. Agric. Water Manage. 168, 23-34. https://doi.org/ 10.1016/j.agwat.2016.01.007